

Gaseous Ions. 3.¹ MINDO/3 Calculations for the Rearrangements of Substituted Benzyl Cations

Michael J. S. Dewar* and David Landman

Contribution from the Department of Chemistry, The University of Texas at Austin, Austin, Texas 78712. Received October 3, 1975

Abstract: MINDO/3 calculations are reported for the rearrangements of substituted benzyl cations to tropylium derivatives, following the mechanism previously deduced for benzyl cation. *p*-Chlorobenzyl cation is predicted to rearrange about as easily as benzyl. The barrier to rearrangement is much higher for *p*-hydroxybenzyl cation, which is probably more stable than hydroxytropylium. The nitro group in *p*-nitrobenzyl cation is orthogonal to the ring, but coplanar in nitrotropylium. The rearrangement of *p*-nitrobenzyl cation to nitrotropylium should be about as easy as that of benzyl, but a competing rearrangement is possible to *p*-nitrobenzyl cation, which can then cleave to NO and semiquinone radical ion. These results are consistent with the experimental evidence.

The mass spectra of cycloheptatriene, toluene, norbornadiene, tropylium salts, and of α -substituted toluenes (PhCH_2X) contain strong peaks corresponding to C_7H_7^+ , commonly attributed to tropylium (**1**). A preceding paper¹ reported MINDO/3 calculations for one of the possible² processes involved, i.e., rearrangement of benzyl cation (**2**) to

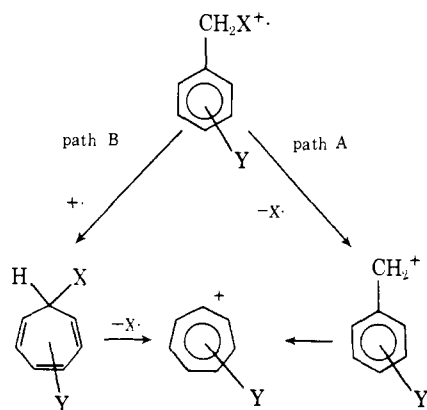


1. Similar rearrangements have also been reported^{3a} for mono (ring)-substituted toluenes, $\text{XC}_6\text{H}_4\text{CH}_3$. Here the formation of C_7H_7^+ probably involves the initial formation of a tolyl cation, and our MINDO/3 calculations¹ showed that these could also rearrange quite easily to **2** and hence to **1**.

In the case of disubstituted toluenes $\text{XC}_6\text{H}_3\text{CH}_2\text{Y}$, with one substituent in the ring and one on the side chain, formation of C_7H_7^+ by unimolecular processes is impossible, since there are not enough hydrogen atoms present. The mass spectra of such species therefore commonly contain peaks corresponding to an ion with the composition $\text{C}_7\text{H}_6\text{X}^+$.

Bursey et al.^{3a} have reviewed these reactions in some detail. It has been suggested^{3b} that they may take place by two distinct paths (Scheme I). In path A, fission of the CX bond leads to

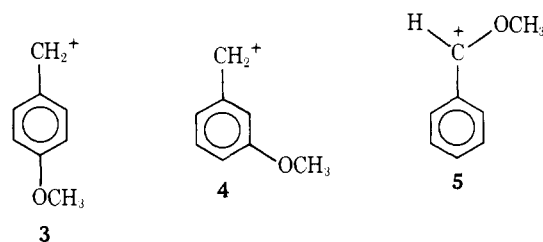
Scheme I



a ring-substituted benzyl cation, which rearranges to tropylium; in path B, the initial molecular ion first rearranges to a disubstituted cycloheptatriene molecular ion, which then loses one of the substituents. The choice of path depends on the relative ease of fission of the CX bond in the initial toluene molecular ion and of rearrangement to the corresponding cy-

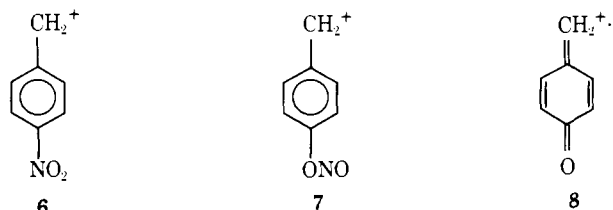
cloheptatriene molecular ion. This mechanism was based on studies^{3b} of appearance potentials and wide-range energy kinetics, which suggested that ions formed at threshold from monosubstituted toluenes $\text{XC}_6\text{H}_4\text{CH}_3$ by loss of hydrogen have a ring-expanded structure in the cases where $\text{X} = \text{CH}_3$, F, or OH, but benzylic structures where $\text{X} = \text{OCH}_3$, SCH_3 , OC_2H_5 , Cl, or Br. On the other hand wide-range electron energy kinetic studies^{3c,d} of the mass spectra of substituted benzyl phenyl ethers, $\text{XC}_6\text{H}_4\text{CH}_2\text{OPh}$, seemed to imply that the ions formed when $\text{X} = \text{CH}_3$, F, Cl, Br, or CF_3 were tropylium derivatives, but benzyl cations when $\text{X} = \text{OCH}_3$ or NO_2 . These results suggest that the nature of a $\text{C}_7\text{H}_6\text{X}^+$ ion may depend on its mode of formation or even the techniques used to study it.

In the case of methoxy, the evidence^{3a} on balance seems to suggest rather strongly that the resulting $(\text{C}_7\text{H}_6\text{OCH}_3)^+$ ion is benzylic, irrespective of the technique used. Bursey et al.^{3a} suggested that the ion is *p*-methoxybenzyl cation (**3**), this being stabilized by the $-\text{E}$ methoxy group at an active position.^{4,5} A $-\text{E}$ substituent should have a much smaller stabilizing effect on the nonalternant tropylium than on the alternant benzyl cation, so it could well displace the equilibrium in favor of the latter. This result seems surprising, since a *m*-methoxy group would be expected to stabilize **2** less than **1**. A likely possibility would be rearrangement of the *m*-methoxybenzyl cation to



α -methoxybenzyl (**5**) via methoxytropylium. In **5** the stabilizing effect of methoxyl should^{4,5} be even greater than in **4**.

The ion from *p*-nitrotoluene also seems to be benzylic.^{3a,e} Here the substituent would destabilize the benzyl cation. Westwood et al.^{6a,b} have suggested that the initially formed *p*-nitrobenzyl cation (**6**) rearranges to the nitrite (**7**), which



then loses nitric oxide. The product would then be the (presumably stable) molecular ion (**8**) of *p*-quinomonomethane.

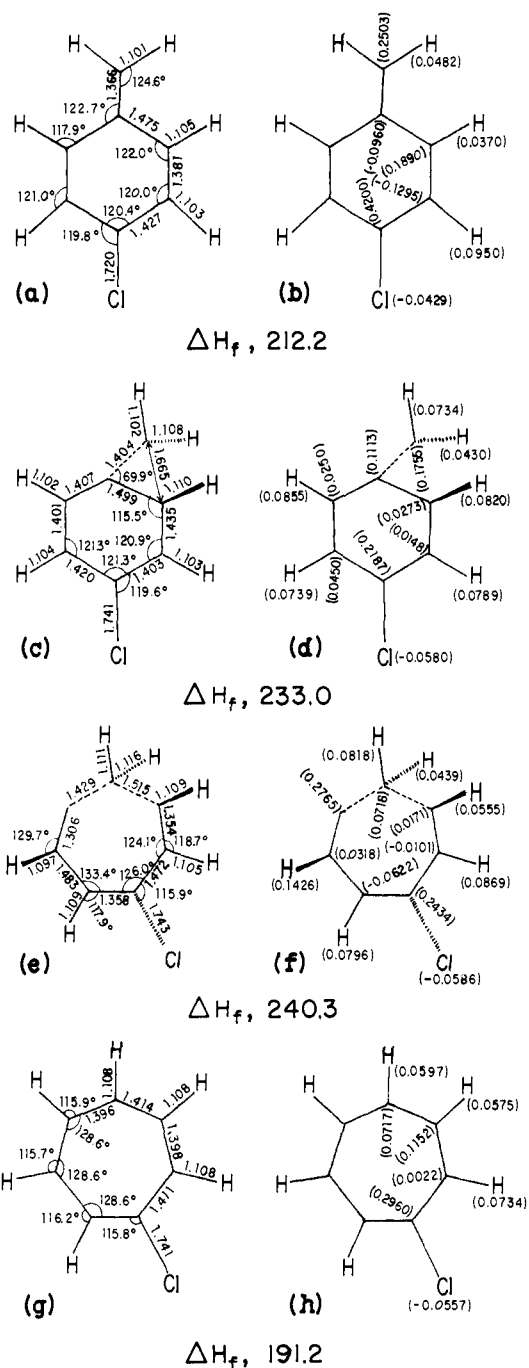
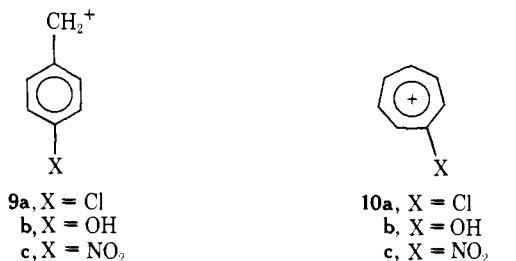


Figure 1. Calculated geometries, heats of formation (ΔH_f , kcal/mol at 25 °C), and distributions of formal charge (a) (b) for **9a**; (c) (d) for **11a**; (e) (f) for **12a**; (g) (h) for **10a**.

Since our MINDO/3 calculations¹ seemed to account quite well for the observed behavior of the $C_7H_7^+$ species, we decided to extend them to the related $C_7H_6X^+$ system. Here we report



a detailed study of the rearrangements of several para-substituted benzyl cations (**9**) to corresponding tropyliums (**10**).

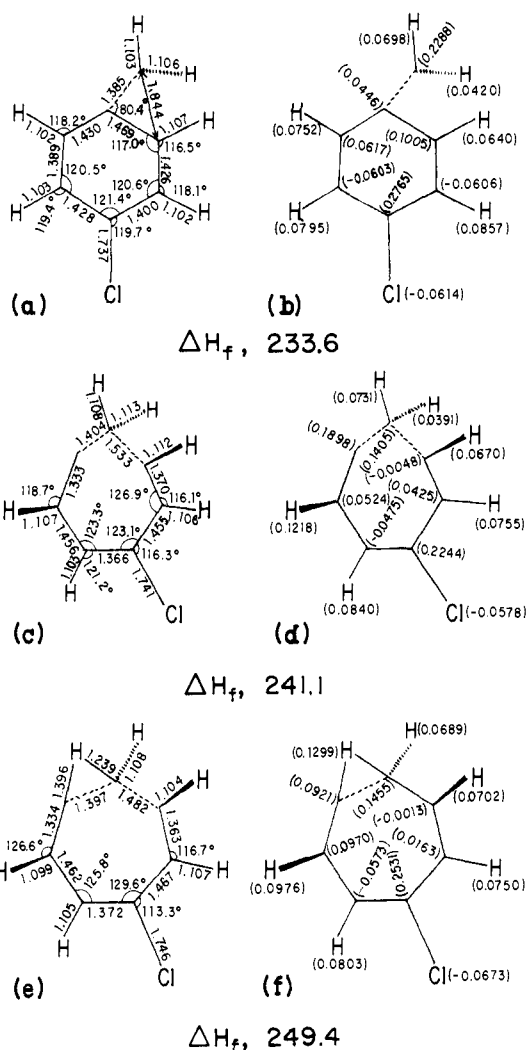


Figure 2. Calculated geometries, heats of formation (ΔH_f , kcal/mol at 25 °C), and distributions of formal charge in the transition states (a) (b) for **9a** \rightarrow **11a**; (c) (d) for **11a** \rightarrow **12a**; (e) (f) for **12a** \rightarrow **10a**.

Procedure

The procedure was the same as that used in the previous study.¹ All geometries were again optimized with respect to all geometrical variables, no assumptions of any kind being made.

Results and Discussion

We first examined the rearrangement of *p*-chlorobenzyl cation (**9a**) to chlorotropylium (**10a**). The reaction was found to follow the same path as that of **2** itself via stable intermediates **11a** and **12a**. The calculated geometries, heats of formation, and distributions of formal charge in the stable species



(**9a**, **10a**, **11a**, and **12a**) are shown in Figure 1, while Figure 2 shows corresponding data for the transition states. Figure 3 represents diagrammatically the MERP (minimum energy reaction path) for the conversion of **9a** to **10a**. The overall activation energy is 37.2 kcal/mol.

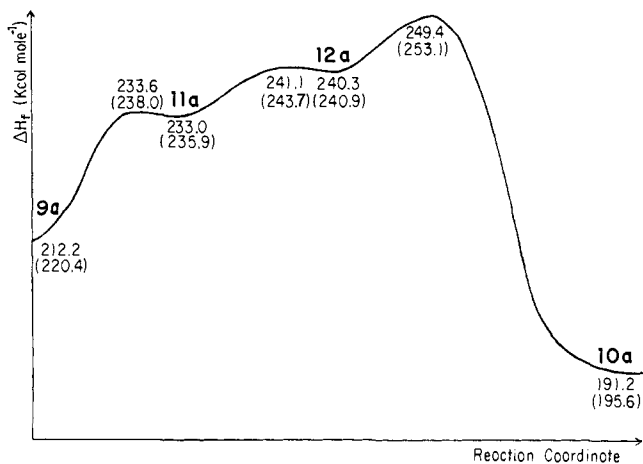
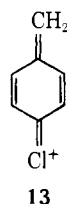


Figure 3. Calculated MERP for $9a \rightarrow 11a \rightarrow 12a \rightarrow 10a$.

The calculated heat of formation of **9a** (212.2 kcal/mol) is in very good agreement with experiment (213 kcal/mol⁷). Since MINDO/3 also gave¹ a good value for **2**, this suggests that it is reproducing well the electronic effects of the chlorine substituent. Therefore, although the value for **10a** is probably too low, like that of **1** (see ref 1), the predicted effects of chlorine on the various heats of reaction are probably reasonably reliable.

The heat of reaction for the overall conversion $9a \rightarrow 10a$ is predicted to be less in magnitude than that for $2 \rightarrow 1$ (-21.0 vs. -24.8 kcal/mol). This is as one would expect. According to PMO theory,⁵ the formal charge at the para position in **2** is the same as in any position in tropylium, i.e., $1/7$; the inductive effect (+I) of chlorine should therefore destabilize both ions equally. However, Cl is also a -E group; the resulting stabilization should be greater⁵ in **9a** than in **10a**. These electronic effects of chlorine can be recognized in Figure 1. The inductive effect leads to a large positive charge at the carbon atom adjacent to chlorine, yet the chlorine atom itself is almost neutral. This is because of the back donation of electrons by π bonding (-E effect); the back donation leads to a decrease in positive charge at the methylene carbon (0.250 vs. 0.274 in **2**) and also to small changes in the lengths of the CC bonds in the ring. Thus C(3,4) and C(4,5) increase in length in comparison with **2** (1.419 Å),¹ while C(2,3) and C(5,6) decrease (length in **2**, 1.385 Å). This corresponds, in resonance terminology, to



contributions by the quinonoid structure **13**. It will be noticed, in agreement with this, that the $\text{CH}_2=\text{C}$ bond is shorter in **9a** than in **2** (1.370 Å)¹.

While, therefore, the chlorine substituent should stabilize the benzyl cation relative to tropylium, the latter (**10a**) should still be the more stable; for the net effect of chlorine is less than even the current experimental value for the difference in energy between **1** and **2** (7 kcal/mol⁷).

The first intermediate, **11a**, is a substituted pentadienyl cation.¹ Here the chlorine is attached at an inactive position in the conjugated C_5^+ system and so should exert no -E effect.⁵ Consequently the heat of reaction for conversion of **9a** to **11a** is greater in magnitude by 5.3 kcal/mol than the corresponding reaction of **2** (-20.8 vs. -15.5¹ kcal/mol). As a result, the activation energy for the reverse reaction $11a \rightarrow 9a$

is very small (0.6 vs. 2.1 kcal/mol in the case of **2**¹), and the asymmetry of the three-membered ring in **11a** is even greater than in the corresponding unsubstituted species (length of the forming C-C bond, 1.665 Å vs. 1.596 Å in the unsubstituted case¹).

The rest of the MERP is quite similar to that for $2 \rightarrow 1$, as one might expect from the arguments given above.

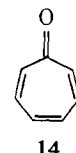
We therefore conclude that the mass spectral behavior of precursors of **9a** should parallel those of precursors of **2**. In both cases the most stable resulting C_7^+ species should be a tropylium ion, i.e., **1** or **10a**.

We next examined the rearrangement of the *p*-hydroxybenzyl cation (**9b**) to hydroxytropylium (**10b**), again⁸ via the corresponding norcaradienyl cation **11b** and the 1-cycloheptatrienyl cation **12b**. In this case, however, the potential surface contained no minimum corresponding to **11b**. The calculated properties of the stable species (**9b**, **10b**, and **12b**) are shown in Figure 4 and those of the transition states in Figure 5. Figure 6 shows diagrammatically the calculated MERP from **9b** to **10b**.

Since the -E effect of hydroxyl is very much greater than that of chlorine,⁴ it is not surprising that the difference between the calculated heats of formation for **9b** and **10b** (15.6 kcal/mol) is much less than that between **2** and **1** (24.8 kcal/mol¹). The decrease is indeed greater than the experimental value for **2** and **1** (7 kcal/mol⁷), so it would not be surprising if **9b** were in fact more stable than **10b**. The strong resonance interactions between hydroxyl and the ring in **9b** are reflected by changes in bond lengths similar to, but greater than, those shown by the chlorine analogue **9a**.

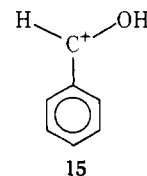
The electromeric effect of chlorine led to an increase in the heat of reaction for the first step in the overall reaction, i.e., $9a \rightarrow 11a$, and a decrease in the reverse activation energy. Here both effects are so much greater that the minimum in the potential surface corresponding to **11b** vanishes, the potential surface containing only an inflexion in this region. The difference in energy between **9b** and **12b** is correspondingly greater than in the unsubstituted case (33.0 vs. 20.5¹ kcal/mol) and the overall activation energy for $9b \rightarrow 10b$ is also very much greater (44.5 vs. 32.7 kcal/mol).

The only other point of interest concerns the structure of **10b**, which is a protonated tropone. As one might expect, the bond lengths in **10b** show a corresponding alternation, although they are still not as completely localized as are the bonds in



tropone (**14**) itself.^{9,10} The distribution of formal charge in **10b** is also entirely different from that in **14**.

Our calculations are therefore consistent with **9b** being a more stable form of the $(\text{C}_7\text{H}_6\text{OH})^+$ ion than **10b**. Since the activation energy for conversion of **9b** to **10b** is also very high, one has a second reason for survival of **9b** as such. However, as we have already noted, there is also the possibility of **10b** undergoing a similar rearrangement to the isomer **15**, i.e.,



protonated benzaldehyde. Figure 4 also shows MINDO/3 results for this species which is seen to be, as expected, more stable than **9b**. Thus, one would in any case expect any precursor of **9b**, or of a corresponding ether, to give rise solely to

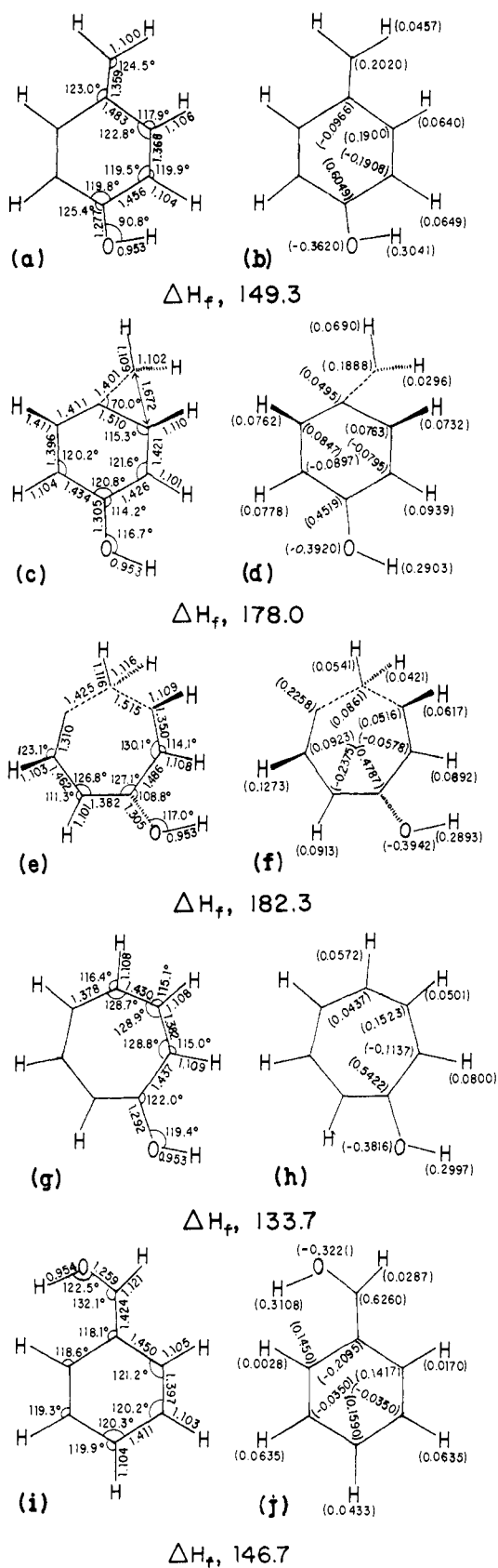


Figure 4. Calculated geometries, heats of formation (ΔH_f , kcal/mol at 25 °C), and distributions of formal charge (a) (b) for **9b**; (c) (d) for **11b**; (e) (f) for **12b**; (g) (h) for **10b**; (i) (j) for **15**.

ions of benzylic type. For either, these will be inhibited from rearranging by the high barriers between them and the corresponding tropylium analogues or, if rearrangement can occur, it can also continue to species such as **5** or **15**, which may

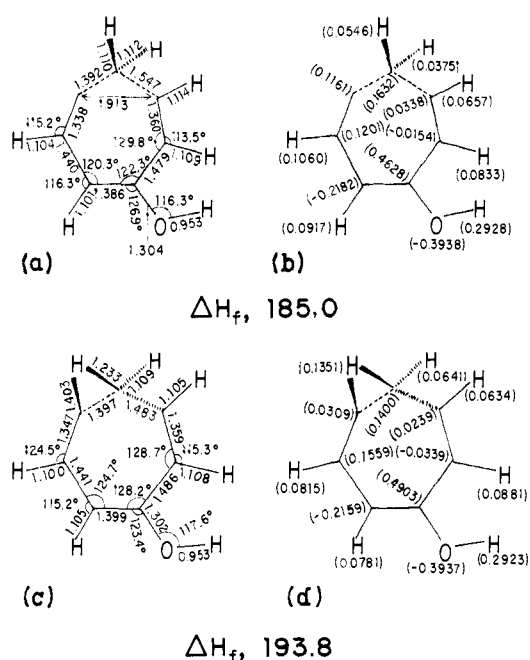


Figure 5. Calculated geometries, heats of formation (ΔH_f , kcal/mol at 25 °C), and distributions of formal charge (a) (b) for **9b** \rightarrow **12b**; (c) (d) for **11b** \rightarrow **10b**.

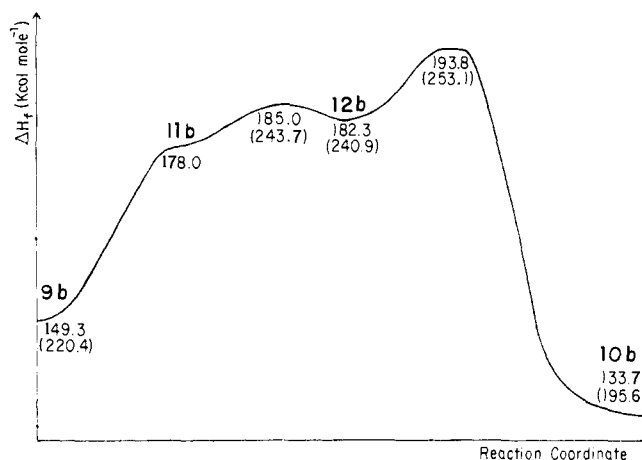


Figure 6. Calculated MERP for **9b** \rightarrow **12b** \rightarrow **10b**.

well be more stable than their tropylium counterparts. We would in any case expect scrambling reactions to be less important in this case than in $C_7H_7^+$ itself, in view of the high barrier to interconversion of **9b** and **10b**.¹¹

Our final study was concerned with the reactions of the *p*-nitrobenzyl cation (**9c**). Here the easiest path to the corresponding tropylium **10c** once again⁸ involved two stable intermediate species, **11c** and **12c**. Their calculated properties are shown in Figure 7 and those of the transition states in Figure 8. Figure 9 shows diagrammatically the MERP for the overall conversion of **9c** to **10c**.

The nitro group has a very powerful +E effect.⁵ When it is attached to a conjugated cation, π interactions between it and the latter will then be very unfavorable. It is therefore not surprising that the nitro group in **9c** is predicted to be orthogonal to the ring, an orientation which completely destroys the π interaction. The geometry of the ring is correspondingly similar to that in **2** itself.

However in **10c**, the nitro group is predicted to lie in the plane of the ring, thus maximizing the π interactions. Why is this? The explanation for this apparent discrepancy is in fact quite simple and rather entertaining.

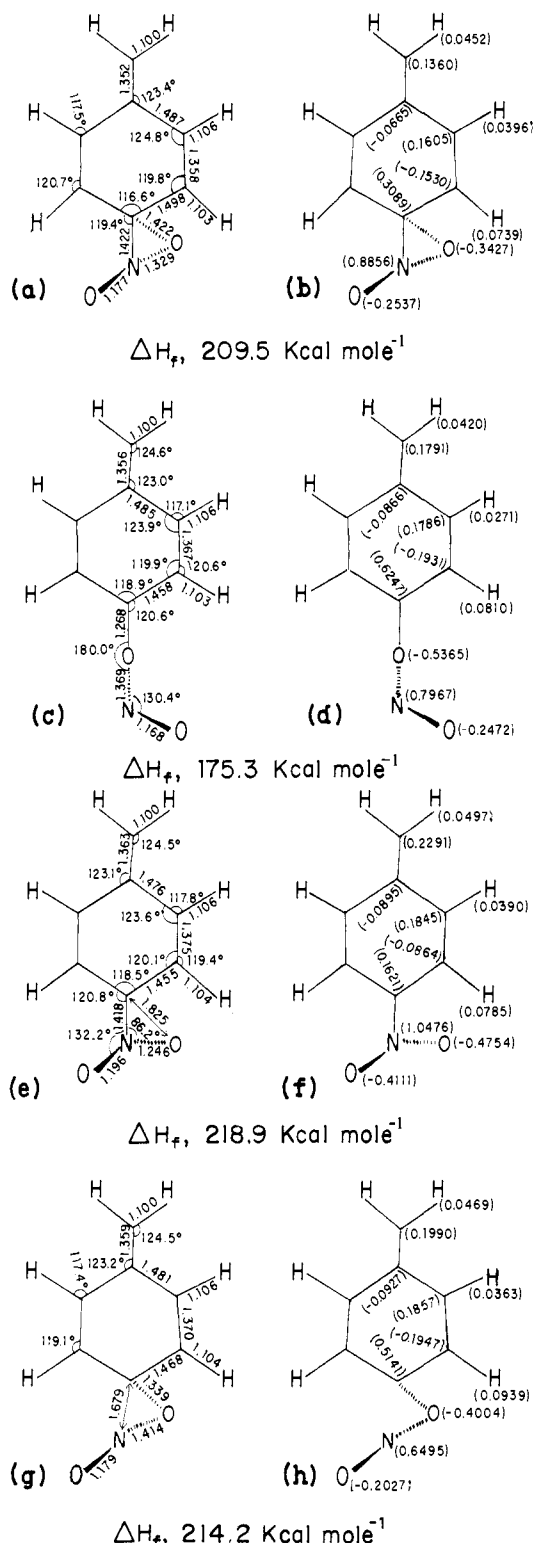


Figure 10. Calculated geometries, heats of formation (ΔH_f), and distributions of formal charge (a) (b) for **16**; (c) (d) for **7**; (e) (f) for the transition state **9c** \rightarrow **16**; (g) (h) for the transition state **16** \rightarrow **7**.

as nitrobenzene are consequently planar, the π interaction between the substituent (NO_2) and the ring having a small but significant net stabilizing effect.

If, however, R is replaced by an odd AH (alternant hydrocarbon^{4,5}) cation such as **2**, the situation is different because such ions have LUMOs that are nonbonding (NBMOs). The interactions between the NBMO of such an ion and the filled bonding MOs of an adjacent $\pm E$ substituent are then about double the bonding–nonbonding interactions in RX' because

the difference in energy between the interacting MOs is only about one-half as great in the former case. The result is a large stabilization in $\text{S}^+\text{X}'$, combined with a transfer of formal positive charge from S^+ to X' . This is seen in **2** itself, regarded as a phenyl derivative of CH_3^+ . The interaction between Ph and CH_2^+ in **2** leads to a large stabilization, combined with a transfer of positive charge from CH_2^+ to the phenyl group.

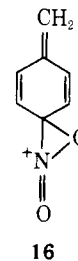
This transfer of positive charge will, however, make replacement of carbon atoms in X' by heteroatoms energetically unfavorable. The net effect of the $+E$ substituent X will therefore depend on a balance between the resulting destabilization and the stabilizing effect of X' . In the case of small $+E$ substituents (such as NO_2) the destabilization wins.^{4,5} The NO_2 group in **6** therefore lies in a plane perpendicular to the ring because this orientation minimizes the unfavorable resonance interaction between them.

The situation changes once again if S^+ is replaced by a nonalternant aromatic ion (T^+) such as tropylium (**1**) or cyclopropenium. The LUMOs in such ions are strongly antibonding,^{4,5} so the interaction between the π MOs of T^+ and those of an adjacent $\pm E$ substituent X' are once more all of bonding–antibonding type. This is why $\pm E$ substituents such as phenyl have little stabilizing effect on such ions,^{4,5} in contrast to their large effect on analogous alternant ones (cf $\text{PhCH}-\text{CH}-\text{CH}_2^+$) and in direct contradiction of resonance theory. It also follows that there should be little transfer of charge between T^+ and X' in $\text{T}^+\text{X}'$, so replacement of carbon atoms in X' by heteroatoms should again have little effect. The π interaction between T^+ and an adjacent $+E$ substituent should therefore be stabilizing and compounds such as **10c** should consequently be coplanar, as our calculations imply.

Since the orthogonal orientation of the nitro group in **9c** suppresses resonance interactions between it and the ring, only the field/inductive effect operates. Since, as we have seen, this should have similar effects in **9**, **10**, and the intermediates **11** and **12**, we would expect the heat of reaction, and overall energy of activation, for **9c** \rightarrow **10c** to be similar to those for **9a** to **10a**. This is the case for the MINDO/3 values, the calculated heats of reaction being -14.7 and -21.0 kcal/mol, respectively, and the calculated activation energies 33.4 and 37.2 kcal/mol, respectively. The calculated MERPs are indeed very similar (cf. Figures 3 and 9).

As noted above, Westwood et al.⁶ have suggested that **9c** (i.e. **6**) may rearrange to **7**, followed by loss of nitric oxide to form **8**. We have also examined this process.

According to our calculations, the conversion of **9c** (**6**) to **7** takes place via a stable intermediate spiro compound (**16**),



rearrangement of this to **7** requiring activation (4.7 kcal/mol). Such spiro compounds have not as yet been isolated as stable species, but there is good evidence for their intervention in both mass spectrometric¹² and photochemical¹³ processes.

The overall activation energy for conversion of **9c** to **7** is predicted to be very low (3.8 kcal/mol). It is true that MINDO/3 tends to overestimate the stabilities of small ring compounds and also of compounds in which adjacent heteroatoms have unshared pairs of electrons in hybrid AOs.¹⁴ Our prediction that **16** is more stable than **9c** is therefore probably incorrect. On the other hand, the difference between the calculated heats of formation of **9c** (**6**) and **7** (39.8 kcal/mol), and

the difference between the calculated activation energies for this process and for $9c \rightarrow 10c$ (29.6 kcal/mol) are much too large to be explained in this way. It therefore seems fairly certain that the conversion of **6** ($9c$) to **7** must be exothermic and that the activation energy for this process must be much less than for $9c \rightarrow 10c$. The calculated MERP for the conversion of $9c$ (**6**) to **7** via **16** is shown in Figure 9 and the calculated properties of **16**, **7**, and the transition states leading to them are given in Figure 10.

Acknowledgment. We are grateful to Dr. C. Cone for helpful discussions concerning this problem. Our work was supported by the Air Force Office of Scientific Research (Grant AFOSR 75-2749) and the Robert A. Welch Foundation (Grant F-126). The calculations were carried out using the CDC 6400/6600 computer at the University of Texas Computation Center. One of us (D.L.) acknowledges the award of a Robert A. Welch Postdoctoral Fellowship.

References and Notes

- (1) Part 1: C. Cone, M. J. S. Dewar, and D. Landman, *J. Am. Chem. Soc.*, **99**, 372 (1977).
- (2) F. W. McLafferty and J. Winkler, *J. Am. Chem. Soc.*, **96**, 5182 (1974).
- (3) (a) For a general reference, see J. T. Bursey, M. M. Bursey, and D. G. I. Kingston, *Chem. Rev.*, **73**, 191 (1973), and references cited therein; (b) J. M. S. Tait, T. W. Shannon, and A. G. Harrison, *J. Am. Chem. Soc.*, **84**, 4 (1962); (c) P. Brown, *ibid.*, **90**, 2694, 4459 (1968); (d) *Org. Mass Spectrom.*, **2**, 1085 (1969); (e) R. H. Shapiro and J. W. Serum, *ibid.*, **2**, 533 (1969).
- (4) M. J. S. Dewar, *J. Am. Chem. Soc.*, **74**, 3355 (1952); "The Molecular Orbital Theory of Organic Chemistry", McGraw-Hill, New York, N.Y., 1969.
- (5) M. J. S. Dewar and R. C. Dougherty, "The PMO Theory of Organic Chemistry", Plenum Publishing Corp., New York, N.Y., 1975.
- (6) (a) R. Westwood, D. H. Williams, and A. N. H. Yeo, *Org. Mass Spectrom.*, **3**, 1485 (1970). (b) This is an example of the general process suggested by Beynon et al. in the molecular ion of nitrobenzene: J. H. Beynon, R. A. Saunders, and A. E. Williams, *Ind. Chim. Belge*, **No. 4**, 311 (1964).
- (7) J. L. Franklin, J. G. Dillard, H. M. Rosenstock, J. T. Herron, K. Draxl, and F. H. Field, *Natl. Stand. Ref. Data Ser., Natl. Bur. Stand.*, **No. 26**, 1 (1969).
- (8) We established that this was again the easiest path from **9** to **10**.
- (9) M. J. S. Dewar and N. Trinajstić, *Croat. Chem. Acta*, **42**, 1 (1970).
- (10) (a) E. Heilbronner and K. Hedberg, *J. Am. Chem. Soc.*, **73**, 1386 (1951); (b) M. Kimura and M. Kubo, *Bull. Chem. Soc. Jpn.*, **26**, 250 (1953); (c) M. Kubo and K. Kimura, *ibid.*, **27**, 455 (1954); (d) K. Kimura, S. Suzuki, M. Kimura, and M. Kubo, *J. Chem. Phys.*, **27**, 320 (1957). (e) K. Kimura, S. Suzuki, M. Kimura, and M. Kubo, *Bull. Chem. Soc. Jpn.*, **31**, 1051 (1958).
- (11) Tait et al.^{3b} have claimed that *p*-hydroxytoluene rearranges to give **10b** in the mass spectrometer, whereas *p*-methoxytoluene gives the *p*-methoxybenzyl cation (**3**). Their evidence, however, was derived entirely from a Hammett-type plot of appearance potentials of $C_7H_6X^+$ ions vs. σ^+ values. Now σ^+ values refer to reactions in solution; here hydrogen bonding to the solvent should greatly increase the σ^+ value of hydroxyl relative to methoxyl. In the gas phase, the effective σ^+ value for hydroxyl should be significantly less than that for methoxyl because the $-I$ effect of methyl in the latter will increase its electron donating power. It therefore seems likely that the deviation of the point for *p*-hydroxytoluene from the line in the plot of Tait et al.^{3b} in fact reflected the use of an inappropriate value for σ^+ .
- (12) (a) M. M. Bursey, *Org. Mass Spectrom.*, **2**, 907 (1969); (b) J. H. Beynon, M. Bertrand, and R. G. Cooks, *J. Am. Chem. Soc.*, **95**, 1739 (1973).
- (13) O. Chapman, D. Heckert, W. Reasoner, and S. Thackaberry, *J. Am. Chem. Soc.*, **88**, 5550 (1966), and references cited therein.
- (14) R. C. Bingham, M. J. S. Dewar, and D. H. Lo, *J. Am. Chem. Soc.*, **97**, 1294, 1302 (1975).

Semiempirical Calculations of Model Oxyheme: Variation of Calculated Electromagnetic Properties with Electronic Configuration and Oxygen Geometry

Robert F. Kirchner and Gilda H. Loew*

Contribution from the Department of Genetics, Stanford University Medical Center, Stanford, California 94305. Received August 26, 1976

Abstract: The iterative extended Hückel method is used to characterize the electronic structure of model oxiferroporphyrin complexes with *N*-methylimidazole as an axial ligand. Twenty-two conformations of the dioxygen ligand are considered. A bent, end-on dioxygen ligand geometry with low energy off-axis displacements and a low energy barrier to rotation about the Fe-O axis possibly coupled to a large amplitude bending mode of the Fe-O-O bond is favored. The electric field gradient at the iron nucleus observed as quadrupole splitting in Mössbauer resonance is calculated for each dioxygen ligand geometry in six likely electronic ground-state configurations. A paired iron(II)-dioxygen configuration yields the large negative electric field gradient observed for oxyhemoglobin and synthesized model compounds. The observed temperature dependence may be accounted for by rotation about the Fe-O axis. Net atomic charges, overlap densities, and variation in iron-ligand interactions as a function of dioxygen ligand geometry as calculated by the iterative extended Hückel method are reported.

Properties attributed to the iron active site of heme proteins have been measured for both oxyhemoglobin and recently synthesized¹ model compounds that show reversible oxygenation. Mössbauer resonance of the proteins² and of the model compounds³ has been used to probe the electron distribution around the iron nucleus. Magnetic susceptibility,⁴ electronic transitions,⁵ and infrared stretching frequencies^{6,7} have been measured in order to further elucidate the binding of dioxygen to iron porphyrins. An x-ray diffraction study of the oxygenated model compound has been performed³ to determine the structure of the iron-dioxygen unit. Yet, despite the large amount of experimental data, two major areas of interest in the complete understanding of oxyhemoglobin remain largely unresolved: (1) differentiation between a formal iron(II)-

dioxygen or iron(III)-superoxide electronic configuration to best describe the interaction of molecular oxygen with the iron porphyrin unit, and (2) determination of the geometry of the dioxygen ligand in the heme pocket, allowing for the possibility of a number of low energy conformations.

Similarities between the electronic spectra of oxyhemoglobin and alkaline met hemoglobin led to the suggestion⁸⁻¹⁰ of a formal iron(III)-superoxide electronic ground-state configuration for oxyhemoglobin. However, the similarities are associated primarily with porphyrin $\pi \rightarrow \pi^*$ transitions.¹¹ Therefore, no direct conclusions can be made regarding the electronic structure of iron and oxygen.¹² More recently three broad transitions in the regions 10 000, 20 000, and 30 000 cm^{-1} were observed in the single crystal polarized absorption